mathematics

MDPI

Article

Loop Soliton Surfaces Generated by the KdV Curve Flow

Ayman Elsharkawy [1,*] and Eman Ghareeb Rezk [2]

[1] Department of Mathematics, Faculty of Science, Tanta University, Tanta 31527, Egypt
[2] Mathematical Science Department, College of Science, Princess Nourah bint Abdlrahman University, P.O. Box 84428, Riyadh 11671, Saudi Arabia; egrezk@pnu.edu.sa
* Correspondence: ayman_ramadan@science.tanta.edu.eg

Abstract

We study the surface swept by the one-soliton solution of the KdV curve flow $\mathbf{r}_t = \frac{1}{2}\kappa^2 T + \kappa_s N$ on unit–speed planar curves. We call the surface swept by this loop soliton the loop soliton surface, and we show that it is a geometric object with some properties, distinct from the flat cylinders of the linearized KdV flow and from the twisted soliton surfaces of the Hasimoto (vortex filament) flow. Workingwith the one-soliton $\kappa = 2B\,\mathrm{sech}(Bu)$, we derive the loop soliton in closed form, compute the first and second fundamental forms of its surface, and establish three properties: the surface is flat ($K = 0$) yet carries non-constant mean curvature $H = -(1 + B^4)\kappa/(2D^{3/2})$, concentrated on a sharp ridge along the loop crossing; all geodesics are affine lines in a flat coordinate system; and the Willmore energy on an infinite strip admits the sharp asymptotics $\mathcal{W} \sim 2BT$ as $B \to 0^+$ and $\mathcal{W} \sim \frac{2}{3}B^7 T$ as $B \to \infty$, a B^7 divergence not exhibited by the linearized KdV cylinder or the Hasimoto one-soliton surface. Three conservation laws inherited from the mKdV hierarchy (via the KdV curve flow, whose curvature equation is of mKdV type; see Remark 2) are identified, a detailed comparison with the linear and Hasimoto frameworks is given, and the non-planar extension, a coupled KdV–mKdV system, is outlined as a challenge for the future.

Keywords: KdV curve flow; loop soliton; planar elastica; mKdV equation; flat surface; mean curvature; Willmore energy; geodesics; Frenet frame; integrable system; conservation laws

MSC: 2020; 53A04; 53A05; 35Q53; 37K10

1. Introduction

The interplay between curve flows and integrable partial differential equations has been a fertile meeting ground for differential geometry, soliton theory, and the calculus of variations for well over half a century [1–3]. The geometric study of surfaces swept by soliton curves occupies a central place in this programme: such surfaces encode in their fundamental forms the full analytic richness of the underlying integrable hierarchy, and their curvature invariants, Gaussian curvature, mean curvature, and Willmore energy, provide coordinate-free fingerprints that distinguish one integrable flow from another [4–7].

Recent years have seen a renewal of this dialogue. On the algebraic side, new integrable structures arising from negative flows of generalized KdV and mKdV hierarchies and their gauge–Miura transformations have been developed [8]. On the geometric side, loop soliton solutions have been constructed for complex space–time-shifted nonlocal short pulse equations [9], integrable systems and invariant curve flows have been studied in symplectic Grassmannian spaces [10], and geometric curve flows in low-dimensional Cayley–Klein geometries have been classified [11]. The defocusing mKdV flow on centroaffine plane

Check for updates

Academic Editor: Süleyman Şenyurt

Received: 3 October 2026
Revised: 31 October 2026
Accepted: 4 November 2026
Published: 6 November 2026

Copyright: © 2026 by the authors. Licensee MDPI, Basel, Switzerland. This article is an open access article distributed under the terms and conditions of the Creative Commons Attribution (CC BY) license.

curves and its relation to KdV dynamics has been analyzed explicitly [12], while integrable geometric flows for curves in pseudoconformal S^3 provide modern comparison points for the non-planar setting [13]. The systematic treatment of boundary value problems for the Euler–Bernoulli planar elastica gives the variational foundation needed to interpret the loop soliton as an energy-minimising curve [14].

Two classical families of curve flows illustrate the range of possibilities. In the linear case, the third-order flow $\mathbf{r}_t = -\mathbf{r}_{sss}$ acts on the curvature by the linearized KdV equation and generates cylindrical surfaces with constant geometric invariants. In the nonlinear case, the Hasimoto flow $\mathbf{r}_t = \mathbf{r}_s \times \mathbf{r}_{ss}$, known as the vortex filament equation, acts on the complex curvature by the nonlinear Schrödinger equation and generates soliton surfaces [7]. Both flows are completely integrable, but they act in fundamentally different ways: the linear flow operates along three consecutive derivatives in the arc length parameter s, while the Hasimoto flow is nonlinear and acts in the binormal direction. Soliton surfaces arising from the nonlinear Schrödinger equation in Minkowski 3-space have been studied in detail in [5], and Hasimoto surfaces within equiform geometry in Minkowski space have been explored in [4]. The geometry of solutions of the quasi-vortex filament equation in Euclidean 3-space $\mathbb{E}^3$ has been analyzed in [6].

The present paper is devoted to a third family, the KdV curve flow

$$\mathbf{r}_t = \tfrac{1}{2}\kappa^2 T + \kappa_s N, \tag{1}$$

where T and N are the Frenet tangent and principal normal, $\kappa = \|\mathbf{r}_{ss}\|$ is the curvature, and $\kappa_s = \partial_s \kappa$. This flow is third order in s, because $N = \mathbf{r}_{ss}/\kappa$ and the term $\kappa_s N$ already involves three derivatives; it operates in the tangent–normal plane, with no binormal component; and it acts on the curvature by the modified Korteweg–de Vries (mKdV) equation

$$\kappa_t = \kappa_{sss} + \tfrac{3}{2}\kappa^2 \kappa_s. \tag{2}$$

This identifies (1) as the geometric lift of the mKdV Equation (2) to curve space. The flow preserves planarity: if $\tau(s,0) = 0$ at time zero, then $\tau(s,t) = 0$ for all subsequent times, and the curve remains in the same plane (see Theorem 1 and [2,15]). Unlike the linear flow, the KdV curve flow is genuinely nonlinear; unlike the Hasimoto flow, it acts in the tangent–normal plane rather than the binormal direction and generates the KdV rather than the NLS hierarchy.

The flow arises in three distinct physical contexts. In planar vortex dynamics, thin vortex tubes confined to a plane evolve according to (1) under the localized induction approximation, so that the curvature profile satisfies KdV and solitons propagate along the filament [2]. Early follow-up work established the systematic link between integrable hierarchies and planar curve motions [3,16,17] and developed Bäcklund transformation tools that are directly relevant to our open problems (Section 10); the core derivation of integrable PDEs, including mKdV, from planar curve motions is given in [1]. In elastic rod mechanics, the planar elastica (Euler's curve of least bending energy $\int \kappa^2 \, ds$ for given arc length and prescribed boundary conditions in the plane) has been studied extensively from the perspectives of stress and material stress [18] and of boundary value problems via an explicit construction procedure [14]; under the KdV curve flow, the elastica evolves by a combination of bending and tension described precisely by (1) [19], and the loop soliton is its exact travelling-wave solution [20,21]. In nonlinear wave theory, KdV models shallow-water gravity waves [22], ion-acoustic solitons in plasmas [23], and the continuum limit of the Fermi–Pasta–Ulam lattice, while the conservation of mass, momentum, and energy in the KdV equation itself has been analyzed systematically by Ali and Kalisch [24]; the complete integrability of KdV, including its Lax pair and infinite conservation laws, is classical [25,26].

A second thread that runs through this work is the geometric analysis of bending energies. The Willmore energy, which arises naturally here as the bending energy of the swept surface, has been the subject of extensive research culminating in the proof of the Willmore conjecture; a comprehensive overview is given by Toda [27]. The closely related total mean curvature functional has been studied for submanifolds of finite type [28], and mean curvature flow, the gradient flow of the area functional, has been the subject of intense activity [29]. The flat surfaces that arise in our analysis also connect to recent work on stability structures and flat surfaces in algebraic geometry [30]. The isothermal coordinate theorem used in Section 6 to guarantee the existence of flat coordinates on our $K = 0$ surface is treated in [31]. Our aim is to determine, in full geometric detail, the surface swept by the simplest travelling wave of the KdV curve flow and to see what role these functionals play in that setting.

Starting from the one-soliton solution $\kappa(s,t) = 2B\,\mathrm{sech}(B(s + B^2t))$ of (2), we derive the tangent angle $\theta(s,t) = 2\arctan(\sinh(B(s+B^2t)))$ and the explicit parametrization of the resulting planar curve, which is the classical loop soliton of the planar elastica [20,21,32]. We then lift this curve to a surface in $\mathbb{E}^3$ by taking the time coordinate as the third spatial dimension, and compute the first and second fundamental forms of the resulting surface in closed form. From these, we obtain the Gaussian and mean curvatures, the shape operator, the principal directions, and the geodesics. Three results are established. First, the surface is flat, $K = 0$, yet its mean curvature is non-constant, given by $H = -(1 + B^4)\kappa/(2D^{3/2})$ with $D = 1 + B^4\sin^2\theta$, so that the surface is a developable with a sharp ridge along the loop crossing that decays exponentially at spatial infinity. Second, all geodesics are affine lines in a globally flat coordinate system (guaranteed by the isothermal coordinate theorem for $K = 0$ surfaces [31]), and the t-parameter curves are simultaneously geodesics and asymptotic lines. Third, the Willmore energy on an infinite strip admits the sharp asymptotics $\mathcal{W} \sim 2BT$ as $B \to 0^+$ and $\mathcal{W} \sim \frac{2}{3}B^7T$ as $B \to +\infty$, a scaling not exhibited by the classical cylinder or the Hasimoto one-soliton surface [7,27]. We further identify three geometric conservation laws inherited from the mKdV hierarchy [25,26], compare our results systematically with the linear and Hasimoto frameworks, and outline the non-planar extension, which leads to a coupled KdV–mKdV system whose geometry remains largely unexplored [8,12,13].

This paper is organized as follows. Section 2 collects the background on Frenet frames, curve flows, and KdV. Section 3 derives the KdV soliton and the loop soliton curve. Section 4 introduces the loop soliton surface and computes the fundamental forms. Section 5 establishes the curvature results. Section 6 classifies geodesics. Section 7 computes and analyzes the Willmore energy, including its asymptotics. Section 8 discusses conservation laws. Section 9 presents worked examples with figures. Section 10 states open problems, including the non-planar coupled KdV–mKdV system.

2. Preliminaries

Let $\alpha : I \to \mathbb{E}^2$ be a unit–speed planar curve with curvature $\kappa > 0$. The Frenet frame $\{T, N\}$ satisfies

$$T' = \kappa N, \qquad N' = -\kappa T, \tag{3}$$

where $'$ denotes ∂_s. Lift to $\mathbb{E}^3$ by $B = (0,0,1)$ (constant binormal). The tangent angle $\theta(s)$ satisfies $\theta' = \kappa$ and $T = (\cos\theta, \sin\theta, 0)$.

For $\mathbf{r} : U \subset \mathbb{R}^2 \to \mathbb{E}^3$, the first and second fundamental forms are

$$\mathrm{I} = E\,ds^2 + 2F\,ds\,dt + G\,dt^2, \quad E = \langle \mathbf{r}_s, \mathbf{r}_s\rangle,\ F = \langle \mathbf{r}_s, \mathbf{r}_t\rangle,\ G = \langle \mathbf{r}_t, \mathbf{r}_t\rangle,$$
$$\mathrm{II} = L\,ds^2 + 2M\,ds\,dt + N_{\mathrm{II}}\,dt^2, \quad L = \langle \mathbf{r}_{ss}, \mathbf{n}\rangle,\ M = \langle \mathbf{r}_{st}, \mathbf{n}\rangle,\ N_{\mathrm{II}} = \langle \mathbf{r}_{tt}, \mathbf{n}\rangle,$$

where $\mathbf{n} = (\mathbf{r}_s \times \mathbf{r}_t)/\|\mathbf{r}_s \times \mathbf{r}_t\|$. The Gaussian and mean curvatures are

$$K = \frac{LN_{\mathrm{II}} - M^2}{EG - F^2}, \qquad H = \frac{EN_{\mathrm{II}} - 2FM + GL}{2(EG - F^2)}.$$

The KdV curve flow and its curvature equation.

Theorem 1 (Goldstein –Petrich [2])**.** *Let $\mathbf{r}(s,t)$ be a smooth unit–speed family of planar curves evolving under (1). Then, the curvature κ satisfies the modified Korteweg–de Vries Equation (2), and the flow preserves planarity ($\tau \equiv 0$ for all t).*

Proof. Write $\mathbf{r}_t = U\,T + V\,N$ where $U = \frac{\kappa^2}{2}$ is the tangential velocity component and $V = \kappa_s$ is the normal velocity component. Since T and N are orthonormal and the flow preserves planarity (the binormal is constant and there is no binormal component in $\mathbf{r}_t$), the time-derivatives of the frame are

$$\partial_t T = a\,N, \qquad \partial_t N = -a\,T, \qquad a := \partial_t T \cdot N. \tag{4}$$

On the other hand,

$$\partial_t T = \partial_t \mathbf{r}_s = \partial_s \mathbf{r}_t = \partial_s(U\,T + V\,N) = (U_s - \kappa V)T + (V_s + \kappa U)N,$$

so comparing the N-component with (4) gives

$$a = V_s + \kappa U. \tag{5}$$

Next, $\kappa = T_s \cdot N$. Differentiating in t and using $T_{st} = T_{ts}$:

$$\kappa_t = (T_t)_s \cdot N + T_s \cdot N_t = \partial_s(a\,N) \cdot N + \kappa N \cdot (-a\,T).$$

Since $N \cdot N_t = 0$ and $N \cdot T = 0$, the second term vanishes, and the first gives

$$\kappa_t = a_s\,N \cdot N + a\,N_s \cdot N = a_s - a\kappa\,T \cdot N = a_s.$$

Substituting (5),

$$\kappa_t = V_{ss} + \kappa_s U + \kappa U_s. \tag{6}$$

With $U = \kappa^2/2$ and $V = \kappa_s$, this is $\kappa_t = \kappa_{sss} + \frac{1}{2}\kappa^2\kappa_s + \kappa^2\kappa_s = \kappa_{sss} + \frac{3}{2}\kappa^2\kappa_s$, which is (2). The binormal component closure and the consistency $\tau \equiv 0$ are verified as in [2,15]. □

Remark 1. *The complete integrability of (2), its Lax pair, inverse scattering, infinite conservation laws, and Bäcklund transformations are classical [25,26], with recent extensions to negative flows of the generalized hierarchy in [8]. The KdV curve flow is thus a completely integrable Hamiltonian system on the space of unit–speed planar curves.*

Remark 2 (The curvature equation is of mKdV type)**.** *We clarify a terminological point. The curvature Equation (2),*

$$\kappa_t = \kappa_{sss} + \tfrac{3}{2}\kappa^2\kappa_s,$$

has a quadratic *nonlinearity $\kappa^2\kappa_s$ and is therefore of* modified *KdV (mKdV) type; the classical KdV equation has the* linear *nonlinearity $\kappa\kappa_s$. The established name "KdV curve flow" for (1) follows Goldstein–Petrich [2], who observed that this flow belongs to the KdV hierarchy via the Miura-type substitution $u = \sqrt{3/2}\,\kappa$, which transforms (2) into the standard mKdV equation $u_t = u_{sss} + u^2 u_s$. We retain the name "KdV curve flow" throughout but stress that the governing curvature equation is mKdV. The conservation laws in Section 8 are the mKdV invariants for κ: under $u = \sqrt{3/2}\,\kappa$, the conserved density $\kappa_s^2 - \frac{1}{4}\kappa^4$ becomes $\frac{2}{3}(u_s^2 - \frac{1}{6}u^4)$, proportional to the standard third mKdV conserved density (see Theorem 10 and Remark 11 below).*

https://doi.org/10.3390/math14214084

3. The KdV Soliton and the Loop Soliton Curve

3.1. The One-Soliton Solution

The one-soliton solution of (2) is

$$\kappa(s,t) = 2B\ \mathrm{sech}\big(B(s+B^2t)\big), \quad B>0. \tag{7}$$

Setting $\eta = B(s+B^2t)$, one verifies directly:

$$\begin{aligned}\kappa_t &= -2B^4\,\mathrm{sech}(\eta)\tanh(\eta),\\ \kappa_{sss}+\tfrac{3}{2}\kappa^2\kappa_s &= -2B^4\,\mathrm{sech}(\eta)\tanh(\eta) \;+\; \tfrac{3}{2}\cdot 4B^2\,\mathrm{sech}^2(\eta)\cdot(-2B^2\,\mathrm{sech}(\eta)\tanh(\eta)) \;+\; \cdots\\ &= \;-2B^4\,\mathrm{sech}(\eta)\tanh(\eta).\end{aligned}$$

The full calculation using $\mathrm{sech}^3\tanh$ terms cancels exactly. The soliton is a right-moving solitary wave of curvature with amplitude $2B$, width $\sim 1/B$, and speed B^2 in the s-direction.

Proposition 1. *The function (7) satisfies the curvature Equation (2) identically (which is of mKdV type; see Remark 2).*

Proof. Set $\eta = B(s+B^2t)$, $c=\mathrm{sech}\,\eta$, $h=\tanh\eta$; then $c'=-ch$, $h'=c^2$, $\eta_s=B$, $\eta_t=B^3$. Hence

$$\kappa_t = -2B^4ch, \tag{8}$$
$$\kappa_s = -2B^2ch, \tag{9}$$
$$\kappa_{ss} = 2B^3c(2h^2-1), \quad (\kappa_{ss}\text{, order } B^3) \tag{10}$$
$$\kappa_{sss} = 2B^4ch\,(5-6h^2) = 2B^4ch\,(6c^2-1), \quad (\kappa_{sss}\text{, order } B^4) \tag{11}$$
$$\tfrac{3}{2}\kappa^2\kappa_s = -12B^4c^3h. \tag{12}$$

Then, using $6c^2h\cdot 2B^4 - 12B^4c^3h = 12B^4c^3h - 12B^4c^3h = 0$ and $-2B^4ch = -2B^4ch$,

$$\begin{aligned}\kappa_{sss}+\tfrac{3}{2}\kappa^2\kappa_s &= 2B^4ch\,(6c^2-1) - 12B^4c^3h\\ &= 12B^4c^3h - 2B^4ch - 12B^4c^3h = -2B^4ch = \kappa_t.\end{aligned}$$

Thus, $\kappa_t = \kappa_{sss}+\frac{3}{2}\kappa^2\kappa_s$, which is (2). □

3.2. Tangent Angle and the Loop Soliton Curve

Proposition 2. *At each fixed time, the curve is determined by its curvature $\kappa(s) = 2B\,\mathrm{sech}(Bs)$ (shifting so that $t=0$). The tangent angle is*

$$\theta(s) = \int_0^s \kappa(s')\,ds' = 2\arctan(\sinh(Bs)). \tag{13}$$

Proof. Freom Equation 7, puting $t=0$ and $s=s'$, we have
$\int_0^s 2B\,\mathrm{sech}(Bs')\,ds' = 2\arctan(\sinh(Bs'))\big|_0^s = 2\arctan(\sinh(Bs))$. □

Useful identities from (13) are setting $c=\mathrm{sech}(Bs)$ and $h=\tanh(Bs)$,

$$\cos\theta = \frac{1-\sinh^2(Bs)}{1+\sinh^2(Bs)} = 2c^2-1, \qquad \sin\theta = \frac{2\sinh(Bs)}{1+\sinh^2(Bs)} = 2ch. \tag{14}$$

Theorem 2 (The loop soliton)**.** *The unit–speed planar curve with curvature $\kappa(s) = 2B\,\mathrm{sech}(Bs)$ and $\theta(0)=0$ has the closed-form parametrization*

$$x(s) = \frac{2\tanh(Bs)}{B} - s, \qquad y(s) = \frac{2}{B}(1-\mathrm{sech}(Bs)). \tag{15}$$

It has the following properties:

(i) *The curvature achieves its maximum* $2B$ *at* $s = 0$.

(ii) *As* $s \to \pm\infty$: $y \to 2/B$ *and* $x \to \pm\infty$, *the curve is asymptotic to the horizontal line* $y = 2/B$ *at both ends.*

(iii) *The curve has vertical tangents* ($\cos\theta = 0$) *at* $Bs = \pm\operatorname{arcsinh}(1)$, *i.e., at* $s = \pm\ln(1+\sqrt{2})/B$, *forming a loop.*

(iv) *Since* $\lim_{s\to+\infty}\theta = \pi$ *and* $\lim_{s\to-\infty}\theta = -\pi$, *the total turning is* $\theta(+\infty) - \theta(-\infty) = \pi - (-\pi) = 2\pi$.

Proof. We integrate the Frenet equations:

$$x(s) = \int_0^s \cos\theta(s')\,ds' = \int_0^s (2\operatorname{sech}^2(Bs') - 1)\,ds' = \frac{2\tanh(Bs)}{B} - s,$$

$$y(s) = \int_0^s \sin\theta(s')\,ds' = \int_0^s 2\operatorname{sech}(Bs')\tanh(Bs')\,ds' = \frac{2}{B}[-\operatorname{sech}(Bs')]_0^s = \frac{2}{B}(1 - \operatorname{sech}(Bs)).$$

For (iii), $\cos\theta = 0$ iff $2c^2 - 1 = 0$ iff $\operatorname{sech}^2(Bs) = 1/2$ iff $\cosh(Bs) = \sqrt{2}$ iff $Bs = \pm\ln(1+\sqrt{2})$. Between these two points, $\cos\theta < 0$ (the tangent points leftward), so the curve turns back on itself, forming a loop. For (iv), $\lim_{s\to\pm\infty}\theta = \pm\pi$, giving total turning 2π. □

Remark 3. *The loop soliton* (15) *is the classical solution of the planar elastica (Euler's curve of least bending energy for given endpoints and tangent conditions) [20,21]; see also [14,18] for modern treatments of the elastica from the perspectives of stress and boundary value problems, respectively. It is also called the* figure-eight *elastica in the literature [32]. The term* figure-eight elastica *refers to the same curve as the loop soliton* (15) *but emphasises its characterisation as a stationary point of the bending energy* $\int \kappa^2\,ds$ *with prescribed endpoints; the self-intersection gives it the appearance of the figure eight. We use* loop soliton *when emphasising the travelling-wave interpretation and* planar elastica *when referring to the class of Euler–Bernoulli bending energy minimisers in the plane. The loop topology—a genuine fold, not a graph over* x*—distinguishes it sharply from the elastica of the stationary VFE soliton (which has no self-intersection) and from any linearized-flow initial curve.*

4. The Loop Soliton Surface

Under the KdV curve flow (1), the one-soliton (7) travels at speed B^2 in the s-direction. In the co-moving frame $u = s + B^2 t$, the curvature is $\kappa(u) = 2B\operatorname{sech}(Bu)$ (time-independent), and the curve retains the shape (15). We lift to $\mathbb{E}^3$ by taking the time coordinate as the third spatial dimension:

$$\mathbf{r}(u,t) = \big(x(u) + B^2 t,\ y(u),\ t\big), \tag{16}$$

where $x(u)$ and $y(u)$ are given by (15), with s replaced by u. The surface $\mathbf{r} : I \times \mathbb{R} \to \mathbb{E}^3$ is parametrized by (u,t).

The First and the Second Fundamental Forms

The partial derivatives of (16) are

$$\mathbf{r}_u = (\cos\theta,\ \sin\theta,\ 0), \qquad \mathbf{r}_t = (B^2,\ 0,\ 1), \tag{17}$$

where $\theta = \theta(u) = 2\arctan(\sinh(Bu))$.

Theorem 3 (First fundamental form)**.** *The first fundamental form of the loop soliton surface* (16) *is*

$$E = 1, \qquad F = B^2\cos\theta, \qquad G = 1 + B^4, \tag{18}$$

with

$$EG - F^2 = 1 + B^4 - B^4\cos^2\theta = 1 + B^4\sin^2\theta =: D. \tag{19}$$

Proof. We compute directly from (17)

$$E = \langle \mathbf{r}_u, \mathbf{r}_u \rangle = \cos^2\theta + \sin^2\theta = 1,$$
$$F = \langle \mathbf{r}_u, \mathbf{r}_t \rangle = B^2 \cos\theta,$$
$$G = \langle \mathbf{r}_t, \mathbf{r}_t \rangle = B^4 + 1.$$

Then, $EG - F^2 = (1 + B^4) - B^4 \cos^2\theta = 1 + B^4(1 - \cos^2\theta) = 1 + B^4 \sin^2\theta$. □

Remark 4. *The factor $D = 1 + B^4 \sin^2\theta$ encodes the loop geometry: $D = 1$ when $\sin\theta = 0$ (at the crossing point $u = 0$ and at $|u| \to \infty$), and $D = 1 + B^4$ when $\sin\theta = 1$ (at the tips of the loop where the tangent is vertical). This variation of the metric discriminant with position is absent in both the linearized and VFE cylinder cases, where $EG - F^2 = \kappa^2 = const$.*

Theorem 4 (Second fundamental form)**.** *The unit normal and second fundamental form of the loop soliton surface are*

$$\mathbf{n} = \frac{1}{\sqrt{D}}(\sin\theta,\ -\cos\theta,\ -B^2 \sin\theta), \tag{20}$$

$$L = -\frac{\kappa}{\sqrt{D}}, \qquad M = 0, \qquad N_{\mathrm{II}} = 0. \tag{21}$$

Proof. We compute $\mathbf{r}_u \times \mathbf{r}_t$:

$$\mathbf{r}_u \times \mathbf{r}_t = (\sin\theta,\ -\cos\theta,\ -B^2 \sin\theta).$$

The magnitude is $\|\mathbf{r}_u \times \mathbf{r}_t\|^2 = \sin^2\theta + \cos^2\theta + B^4 \sin^2\theta = 1 + B^4 \sin^2\theta = D$, so $\mathbf{n} = (\sin\theta, -\cos\theta, -B^2 \sin\theta)/\sqrt{D}$.

The second derivatives are

$$\mathbf{r}_{uu} = (-\sin\theta,\ \cos\theta,\ 0) \cdot \theta' = \kappa(-\sin\theta,\ \cos\theta,\ 0),$$
$$\mathbf{r}_{ut} = \mathbf{0}, \qquad \mathbf{r}_{tt} = \mathbf{0}.$$

(Here, $\theta' = \kappa$ and $\mathbf{r}_{ut} = \partial_t(\cos\theta, \sin\theta, 0) = 0$ since $\theta = \theta(u)$ has no t-dependence.), projecting

$$L = \langle \mathbf{r}_{uu}, \mathbf{n} \rangle = \kappa \langle (-\sin\theta, \cos\theta, 0),\ (\sin\theta, -\cos\theta, -B^2 \sin\theta) \rangle / \sqrt{D}$$
$$= \kappa(-\sin^2\theta - \cos^2\theta)/\sqrt{D} = -\kappa/\sqrt{D},$$
$$M = \langle \mathbf{r}_{ut}, \mathbf{n} \rangle = 0, \qquad N_{\mathrm{II}} = \langle \mathbf{r}_{tt}, \mathbf{n} \rangle = 0.$$

□

5. Curvatures and Shape Operator

Theorem 5 (Gaussian and mean curvatures)**.** *The Gaussian and mean curvatures of the loop soliton surface are*

$$K = 0, \tag{22}$$

$$H = -\frac{(1 + B^4)\,\kappa(u)}{2\,D^{3/2}} = -\frac{(1 + B^4) \cdot 2B\ \mathrm{sech}(Bu)}{2\,(1 + B^4 \sin^2\theta)^{3/2}}. \tag{23}$$

The surface is flat with non-constant mean curvature concentrated at the soliton core $u = 0$ and decaying exponentially as $|u| \to \infty$.

Proof. With $L = -\kappa/\sqrt{D}$, $M = 0$, $N_{\mathrm{II}} = 0$, and $EG - F^2 = D$:

$$K = \frac{LN_{\mathrm{II}} - M^2}{EG - F^2} = \frac{0}{D} = 0.$$

For the mean curvature, we recall $E = 1$, $F = B^2 \cos\theta$, $G = 1 + B^4$:

$$H = \frac{E N_{\mathrm{II}} - 2F M + G L}{2(EG - F^2)} = \frac{0 - 0 + (1 + B^4)(-\kappa/\sqrt{D})}{2D} = -\frac{(1 + B^4)\kappa}{2D^{3/2}}.$$

Since $\kappa = 2B\,\mathrm{sech}(Bu)$ and $\sin^2\theta = 4\,\mathrm{sech}^2(Bu)\tanh^2(Bu) \to 0$ as $|u| \to \infty$, both κ and $D - 1$ decay exponentially, so $H \to 0$ exponentially. □

Remark 5. *At the loop apex $u = 0$: $\theta = 0$, $\sin\theta = 0$, $D = 1$, $\kappa = 2B$, so $H(0) = -(1 + B^4)B$. At the tips $\sin\theta = 1$, $D = 1 + B^4$, $\kappa = 2B\,\mathrm{sech}(Bu^*)$ for some $u^* > 0$:*

$$H(u^*) = -\frac{(1 + B^4) \cdot 2B\,\mathrm{sech}(Bu^*)}{2(1 + B^4)^{3/2}} = -\frac{B\,\mathrm{sech}(Bu^*)}{(1 + B^4)^{1/2}},$$

which is smaller in magnitude than $H(0)$. The mean curvature is therefore largest at the crossing point of the loop and decays toward the loop tips and to zero at spatial infinity.

Theorem 6 (Shape operator and principal curvatures)**.** *The principal curvatures of the loop soliton surface are*

$$\lambda_1 = -\frac{\kappa}{\sqrt{D}}, \qquad \lambda_2 = 0. \tag{24}$$

The corresponding principal directions are $\mathbf{r}_u$ (tangent to the u-parameter curves) and the direction $\mathbf{r}_t - F\mathbf{r}_u/E$ (perpendicular to $\mathbf{r}_u$ in the tangent plane). The surface is developable with one non-zero principal curvature equal to $-\kappa/\sqrt{D}$.

Proof. Since $\mathrm{II} = L\,du^2$ (with $M = N_{\mathrm{II}} = 0$), the shape operator $\mathcal{S} = (\mathrm{I}^{-1}) \cdot \mathrm{II}$ is diagonal with $\mathcal{S}(\mathbf{r}_u) = \lambda_1 \mathbf{r}_u$ and $\mathcal{S}(\mathbf{v}) = 0$ for $\mathbf{v} = \mathbf{r}_t - F\mathbf{r}_u$ (the vector perpendicular to $\mathbf{r}_u$ in the tangent plane). The eigenvalue is $\lambda_1 = L/E = -\kappa/\sqrt{D}$. □

Corollary 1 (Asymptotic and curvature lines)**.** *On the loop soliton surface:*

(i) The t-parameter curves ($u = $ const) are asymptotic lines*: $\mathrm{II}(v, v) = N_{\mathrm{II}}\,dt^2 = 0$.*

(ii) The u-parameter curves ($t = $ const) are lines of curvature *with principal curvature $\lambda_1 = -\kappa/\sqrt{D}$.*

Proof. (i) For $du = 0$: $\mathrm{II} = N_{\mathrm{II}}\,dt^2 = 0$. (ii) Along u-curves: $\mathrm{II} = L\,du^2 = (-\kappa/\sqrt{D}) \cdot \mathrm{I}|_{dt=0}$ (restricted to $dt = 0$), confirming $\lambda_1 = -\kappa/\sqrt{D}$. □

6. Geodesics

Theorem 7 (Geodesics of the loop soliton surface)**.** *The loop soliton surface has Gaussian curvature $K = 0$ everywhere and is therefore locally isometric to the Euclidean plane; by the theorem on isothermal coordinates, flat coordinates exist in which geodesics appear as straight lines. In the (u, t)-parametrization, the geodesics of the loop soliton surface satisfy*

$$\ddot{u} = -\frac{B^4 \kappa \sin\theta\cos\theta}{D}\,\dot{u}^2, \qquad \ddot{t} = \frac{B^2 \kappa \sin\theta}{D}\,\dot{u}^2, \tag{25}$$

where $\kappa = \kappa(u) = 2B\,\mathrm{sech}(Bu)$, $\theta = \theta(u) = 2\arctan(\sinh(Bu))$, and $D = 1 + B^4 \sin^2\theta$. In the small-amplitude limit $B \to 0$, every geodesic reduces to an affine line $u(\lambda) = u_0 + p\lambda$, $t(\lambda) = t_0 + q\lambda$ with $u_0, t_0, p, q \in \mathbb{R}$.

Proof. The loop soliton surface is parametrized by (16), with metric coefficients computed in Theorem 3:

$$(g_{11}, g_{12}, g_{22}) = (E, F, G) = (1,\ B^2 \cos\theta,\ 1 + B^4),$$

where $x^1 = u$ and $x^2 = t$. Since $K = 0$ by Theorem 5, the surface is locally isometric to the Euclidean plane (isothermal-coordinate theorem, see [31], geodesics appear as straight lines in flat coordinates. To obtain the geodesic equations in the (u, t)-chart, we compute the Christoffel symbols $\Gamma^k_{ij} = \frac{1}{2} g^{kl}(\partial_i g_{jl} + \partial_j g_{il} - \partial_l g_{ij})$ explicitly.

Among the three metric components, only $F = g_{12} = B^2 \cos\theta(u)$ depends on a coordinate; it depends on u alone. Hence the only non-zero partial derivative of any g_{ij} is

$$\partial_u F = -B^2 \sin\theta\, \theta'(u) = -B^2 \kappa \sin\theta, \tag{26}$$

using $\theta' = \kappa$. All other derivatives vanish: $\partial_t g_{ij} = 0$ for every i, j, and $\partial_u g_{11} = \partial_u g_{22} = 0$ since $E = 1$ and $G = 1 + B^4$ are constant.

The determinant of the metric is

$$\det g = EG - F^2 = 1 + B^4 - B^4 \cos^2\theta = 1 + B^4 \sin^2\theta =: D,$$

and $D \geq 1 > 0$ everywhere. Therefore

$$g^{11} = \frac{G}{D} = \frac{1 + B^4}{D}, \qquad g^{12} = g^{21} = -\frac{F}{D} = -\frac{B^2 \cos\theta}{D}, \qquad g^{22} = \frac{E}{D} = \frac{1}{D}.$$

Because the only non-vanishing derivative of any g_{ij} is $\partial_u g_{12} = \partial_u F$, most symbols vanish identically. For the remaining two we have, using $\partial_u g_{11} = \partial_u g_{22} = \partial_u g_{uu} = \partial_u g_{tt} = 0$ and $\partial_t g_{ij} = 0$:

$$\begin{aligned}
\Gamma^u_{uu} &= \tfrac{1}{2} g^{uu} \cdot 0 + \tfrac{1}{2} g^{ut}\big(2\partial_u g_{ut} - \partial_u g_{tt}\big) = g^{ut}\, \partial_u F, \\
\Gamma^t_{uu} &= \tfrac{1}{2} g^{tu} \cdot 0 + \tfrac{1}{2} g^{tt}\big(2\partial_u g_{ut} - \partial_u g_{uu}\big) = g^{tt}\, \partial_u F, \\
\Gamma^u_{ut} &= \tfrac{1}{2} g^{uu} \partial_t g_{11} + \tfrac{1}{2} g^{ut}\big(\partial_u g_{11} + \partial_t g_{12} - \partial_u g_{12}\big) = 0, \\
\Gamma^t_{ut} &= \tfrac{1}{2} g^{tu} \partial_t g_{11} + \tfrac{1}{2} g^{tt}\big(\partial_u g_{22} + \partial_t g_{12} - \partial_t g_{22}\big) = 0,
\end{aligned}$$

and similarly $\Gamma^u_{tt} = \Gamma^t_{tt} = 0$ (all their terms involve t-derivatives or u-derivatives of the constant entries g_{11}, g_{22}). Substituting the inverse-metric entries and the value of $\partial_u F$ from (26):

$$\begin{aligned}
\Gamma^u_{uu} &= -\frac{B^2 \cos\theta}{D} \cdot \big(-B^2 \kappa \sin\theta\big) = \frac{B^4 \kappa \sin\theta \cos\theta}{D}, \\
\Gamma^t_{uu} &= \frac{1}{D} \cdot \big(-B^2 \kappa \sin\theta\big) = -\frac{B^2 \kappa \sin\theta}{D}.
\end{aligned}$$

With all symbols except Γ^u_{uu} and Γ^t_{uu} vanishing, the geodesic equations $\ddot{x}^k + \Gamma^k_{ij} \dot{x}^i \dot{x}^j = 0$ reduce to

$$\ddot{u} + \Gamma^u_{uu}\, \dot{u}^2 = 0, \qquad \ddot{t} + \Gamma^t_{uu}\, \dot{u}^2 = 0,$$

which is exactly (25).

As $B \to 0$, we have $F = B^2 \cos\theta \to 0$ and $D \to 1$ uniformly. Moreover, $\theta(u) = 2 \arctan(\sinh(Bu)) \to 0$ uniformly on compact u-sets, hence $\sin\theta \to 0$. Both right-hand sides of (25) therefore tend to zero, and the geodesic equations reduce to $\ddot{u} = \ddot{t} = 0$. Their solutions are affine lines $u(\lambda) = u_0 + p\lambda$, $t(\lambda) = t_0 + q\lambda$. □

Remark 6. *Let $G := 1 + B^4$, $D := 1 + B^4 \sin^2\theta$. The map*

$$\xi(u, t) = \int_0^u \sqrt{D/G}\, ds, \qquad \eta(u, t) = \sqrt{G}\, t + \frac{1}{\sqrt{G}} \int_0^u F(s)\, ds$$

satisfies $d\xi^2 + d\eta^2 = E\, du^2 + 2F\, du\, dt + G\, dt^2 = ds^2$ (using $D + F^2 = EG = G$). Hence (ξ, η) are global flat coordinates and geodesics are straight lines $\xi = \xi_0 + p\lambda$, $\eta = \eta_0 + q\lambda$. Consequently,

(i) the t-curves map to vertical lines and are geodesics, matching Corollary 1;
(ii) any geodesic with $p \neq 0$ has $\xi \to \pm\infty$, hence $u \to \pm\infty$;
(iii) the u-curves are geodesics only when $F/\sqrt{D}$ is constant, i.e., only in the limits $u \to \pm\infty$, where they become tangent to the geodesic field.

7. Willmore Energy and Its Asymptotics

7.1. Exact Formula

Theorem 8 (Willmore energy: exact integrand)**.** *The Willmore energy of the loop soliton surface on the strip* $[-S, S] \times [0, T]$ *is*

$$\mathcal{W}(S, T) = T \int_{-S}^{S} H^2 \sqrt{EG - F^2}\, du = T \int_{-S}^{S} \frac{(1 + B^4)^2\, \kappa(u)^2}{4\, D^{5/2}}\, du, \tag{27}$$

where $\kappa(u) = 2B\,\mathrm{sech}(Bu)$ *and* $D = 1 + B^4 \sin^2\theta(u)$*. The integral is finite for all* $S < \infty$*.*

Proof. Using $H^2 = \kappa^2(1 + B^4)^2/(4D^3)$ and $\sqrt{EG - F^2} = \sqrt{D}$:

$$H^2\sqrt{EG - F^2} = \frac{(1 + B^4)^2\kappa^2}{4D^3} \cdot \sqrt{D} = \frac{(1 + B^4)^2\kappa^2}{4D^{5/2}}.$$

Since $\kappa = 2B\,\mathrm{sech}(Bu)$ decays exponentially and $D \geq 1$, the integrand decays as $\mathrm{sech}^2(Bu)$ and is integrable on $\mathbb{R}$. The t-integral is trivial since the integrand is t-independent (the curve shape is frozen in the co-moving frame). □

7.2. Rigorous Asymptotics via Laplace's Method

We now resolve the asymptotic behaviour of the Willmore energy in both limits. The key observation is that the integral (27) is a Laplace-type integral whose dominant contribution comes from the boundary layer at $u = 0$ for large B and from the entire real line uniformly for small B.

Theorem 9 (Willmore energy asymptotics)**.** *Let* $\mathcal{W}(\infty, T) = \lim_{S\to\infty} \mathcal{W}(S, T)$ *denote the total Willmore energy on the infinite strip.*

(a) Small-amplitude limit. As $B \to 0^+$*,*

$$\mathcal{W}(\infty, T) = 2BT + O(B^5). \tag{28}$$

(b) Large-amplitude limit. As $B \to +\infty$*, the leading asymptotic expansion is*

$$\mathcal{W}(\infty, T) = \frac{2}{3}B^7T + \frac{35}{24}B^3T + O(B^{-1}). \tag{29}$$

In particular $\mathcal{W}(\infty, T) \sim \frac{2}{3}B^7T$ *to leading order.*

(c) Uniform boundedness. For every fixed $B > 0$*, the integral* (27) *converges and* $\mathcal{W}(\infty, T) < \infty$*.*

Proof. (a) Small B. For small B, both $B^4 \to 0$ and $D - 1 = B^4 \sin^2\theta \to 0$. Expand the integrand:

$$\frac{(1 + B^4)^2\kappa^2}{4D^{5/2}} = B^2\,\mathrm{sech}^2(Bu)\,(1 + B^4)^2\left(1 - \tfrac{5}{2}B^4\sin^2\theta + \ldots\right).$$

Integrating term by term:

$$\mathcal{W}(\infty, T) = TB^2\int_{-\infty}^{\infty} \mathrm{sech}^2(Bu)\, du + O(B^6) = TB^2 \cdot \frac{2}{B} + O(B^6) = 2BT + O(B^6),$$

using $\int_{-\infty}^{\infty} \mathrm{sech}^2(Bu)\, du = 2/B$. This establishes (28).

(b) Large B.

$$\mathcal{W}(\infty, T) = T(1 + B^4)^2B^2\int_{-\infty}^{\infty} \frac{\mathrm{sech}^2(Bu)}{D(u)^{5/2}}\, du.$$

Set $v = Bu$, so $du = dv/B$ and $D(u) = 1 + 4B^4 \operatorname{sech}^2 v \tanh^2 v$. Then

$$\mathcal{W}(\infty, T) = T(1 + B^4)^2 B \int_{-\infty}^{\infty} \frac{\operatorname{sech}^2 v}{(1 + 4B^4 \operatorname{sech}^2 v \tanh^2 v)^{5/2}} \, dv.$$

The integrand is concentrated in the boundary layer $|v| \lesssim B^{-2}$.

More precisely, for $|v| \geq MB^{-2}$ with M fixed, we have $4B^4 \operatorname{sech}^2 v \tanh^2 v \geq CB^4 e^{-4|v|}$ for some $C > 0$, so the integrand is bounded by $\operatorname{sech}^2 v / (CB^4 e^{-4|v|})^{5/2}$, which is integrable and contributes $O(B^{-10})$ to the integral, negligible compared to the B^{-2} leading term.

In the inner region, expand $\operatorname{sech}^2 v = 1 + O(v^2)$ and $\tanh^2 v = v^2 + O(v^4)$. Rescale $v = B^{-2} w$; then,

$$4B^4 \operatorname{sech}^2 v \tanh^2 v = 4w^2 + O(B^{-4} w^4), \qquad dv = B^{-2} dw,$$

so the leading contribution to the integral is

$$B^{-2} \int_{-\infty}^{\infty} \frac{dw}{(1 + 4w^2)^{5/2}} = B^{-2} \cdot \frac{2}{3},$$

using the elementary evaluation $\int_{-\infty}^{\infty} (1 + 4w^2)^{-5/2} dw = \frac{2}{3}$ (obtained by $2w = \tan \psi$).

Substituting back, we have

$$\mathcal{W}(\infty, T) \sim \tfrac{2}{3} T(1 + B^4)^2 B \cdot B^{-2} = \tfrac{2}{3} T(1 + B^4)^2 B^{-1}.$$

Expanding $(1 + B^4)^2 = 1 + 2B^4 + B^8$, we have

$$\mathcal{W}(\infty, T) \sim \tfrac{2}{3} T\big(B^7 + 2B^3 + B^{-1}\big).$$

To obtain the next-order term, we carry the inner-region expansion to $O(B^{-4})$. Using the Taylor series

$$\operatorname{sech}^2 v \cdot \tanh^2 v = v^2 - \tfrac{5}{3} v^4 + O(v^6),$$

the substitution $v = B^{-2} w$ gives

$$4B^4 \operatorname{sech}^2 v \tanh^2 v = 4w^2 - \tfrac{20}{3} B^{-4} w^4 + O(B^{-8}).$$

Expanding the denominator and the numerator $\operatorname{sech}^2 v = 1 - B^{-4} w^2 + O(B^{-8})$, the integrand in the inner region becomes

$$\frac{1}{(1 + 4w^2)^{5/2}} + B^{-4} \left[\frac{-w^2}{(1 + 4w^2)^{5/2}} + \frac{\frac{50}{3} w^4}{(1 + 4w^2)^{7/2}} \right] + O(B^{-8}).$$

Using the standard evaluations $\int_{-\infty}^{\infty} w^2 (1 + 4w^2)^{-5/2} dw = \frac{1}{12}$ and $\int_{-\infty}^{\infty} w^4 (1 + 4w^2)^{-7/2} dw = \frac{1}{80}$, the correction integral is

$$I_1 = -\frac{1}{12} + \frac{50}{3} \cdot \frac{1}{80} = -\frac{1}{12} + \frac{5}{24} = \frac{1}{8}.$$

Hence the inner integral equals $B^{-2}\big(\frac{2}{3} + \frac{1}{8} B^{-4} + O(B^{-8})\big)$, and

$$\begin{aligned} \mathcal{W}(\infty, T) &= T(1 + B^4)^2 B \cdot B^{-2} \left(\frac{2}{3} + \frac{1}{8B^4} \right) + O(B^{-1}) \\ &= \frac{2}{3} T \, \frac{(1 + B^4)^2}{B} + \frac{T}{8} \, \frac{(1 + B^4)^2}{B^5} + O(B^{-1}). \end{aligned}$$

Expanding $(1 + B^4)^2 = B^8 + 2B^4 + 1$, the B^3 contributions from both terms are $\frac{2}{3} \cdot 2B^3 + \frac{1}{8} \cdot B^3 = \frac{4}{3} B^3 + \frac{1}{8} B^3 = \frac{35}{24} B^3$, giving

$$\mathcal{W}(\infty, T) = \frac{2}{3} B^7 T + \frac{35}{24} B^3 T + O(B^{-1}),$$

which is (29). (Note that no B^5 term can arise at this order: the prefactor $(1 + B^4)^2 B$ contributes only powers B^9, B^5, B^1, while the inner integral expansion contributes only even *negative* powers of B, so their product contains no B^5 term.)

(c) Convergence for fixed B follows from the exponential decay $\operatorname{sech}^2(Bu) \to 0$ as $|u| \to \infty$ and the lower bound $D \geq 1$. □

Remark 7 (Interpretation). *The two limits are qualitatively very different. In the small-amplitude limit $B \to 0^+$, the surface degenerates toward the flat plane swept at infinitesimal speed: the loop broadens without bound ($y_\infty = 2/B \to \infty$), and the mean curvature vanishes uniformly. In the large-amplitude limit $B \to +\infty$, the surface develops a sharp boundary-layer ridge concentrated at $u = 0$; the mean curvature peak scales as $|H(0)| = (1 + B^4)B \sim B^5$ as $B \to +\infty$ (in the sense that $|H(0)|/B^5 \to 1$ as $B \to +\infty$), and its support shrinks as B^{-2}. The Willmore energy thus diverges as B^7, precisely because the growth B^{10} of H^2 is only partially compensated by the shrinking width B^{-2}, leaving a net B^7 divergence.*

The physical interpretation is that the loop soliton becomes an increasingly sharp "corner" of the surface as B increases, and the bending energy concentrates in an ever-thinner neighbourhood of the corner, dominating the integral in the limit.

Remark 8 (Novelty relative to generalised cylinders). *We clarify which properties of the loop soliton surface are genuinely specific to the KdV flow and which hold for* all *generalised cylinders (surfaces swept by translating a fixed planar curve in a fixed direction). Any generalised cylinder satisfies $K = 0$, has its rulings as geodesics and asymptotic lines, and admits a globally flat coordinate system. These properties therefore do not constitute novel results in themselves.*

The following are genuinely new in our setting:

(i) *The mean curvature formula $H = -(1 + B^4)\kappa/(2D^{3/2})$ with the* position-dependent *factor $D = 1 + B^4 \sin^2\theta$, which is absent for classical cylinders (where D is constant and H is constant along each ruling).*

(ii) *The sech-driven concentration of $|H|$ in a ridge of width $\sim B^{-1}$ and amplitude $\sim B^5$ at the loop crossing, decaying exponentially to zero at spatial infinity.*

(iii) *The B^7 divergence of the Willmore energy, which arises from the $D^{5/2}$ denominator and the KdV soliton amplitude scaling and which is not produced by any classical cylinder or NLS soliton surface.*

Remark 9 (Comparison with other frameworks). *The Willmore asymptotics distinguishes the KdV loop soliton from both comparison frameworks:*

- *For the linearized cylinder, the Willmore energy diverges linearly in the strip length because H is constant along the surface.*
- *For the VFE stationary soliton (Hasimoto flow), the Willmore integral reduces to an elementary combination of sech–powers, is therefore finite, and carries no position-dependent factors; its B-dependence is fixed by the sech–integral alone.*
- *For the KdV loop soliton, the Willmore energy is finite but non-elementary: its large-B asymptotics is $B^7 T$, a genuinely new scaling that reflects the loop topology through the $D^{5/2}$ denominator. This places the KdV case in a distinct position within the broader theory of Willmore functionals [27].*

8. Conservation Laws

Theorem 10 (Geometric conservation laws). *Under the KdV curve flow (1), the following three geometric quantities are conserved for all t (for curves with suitable decay at infinity):*

(i) *Total turning : $\mathcal{I}_0 = \int_{-\infty}^{\infty} \kappa \, ds = \theta(+\infty) - \theta(-\infty) = 2\pi$ for the loop soliton.*

(ii) Elastica energy (first nontrivial mKdV invariant): $\mathcal{I}_1 = \int_{-\infty}^{\infty} \kappa^2\, ds$.

(iii) Second mKdV invariant:

$$\mathcal{I}_2 = \int_{-\infty}^{\infty} \left(\kappa_s^2 - \tfrac{1}{4}\kappa^4\right) ds.$$

The coefficient $-\frac{1}{4}$ *is the unique value making* $\mathcal{I}_2$ *conserved: integrating by parts (boundary terms vanish by the assumed decay) gives*

$$\frac{d}{dt}\int \kappa_s^2\, ds = 3\int \kappa\kappa_s^3\, ds, \qquad \frac{d}{dt}\int \kappa^4\, ds = 12\int \kappa\kappa_s^3\, ds,$$

so $\frac{d}{dt}\int(\kappa_s^2 - c\kappa^4)\, ds = (3 - 12c)\int \kappa\kappa_s^3\, ds = 0$ *if and only if* $c = \frac{1}{4}$.

These are the images under the Goldstein–Petrich map [2] of the standard mKdV conserved densities (see Remarks 2 and 11). The mKdV hierarchy has infinitely many conservation laws, but the higher ones involve κ_s, κ_{ss}, *etc., not simply powers* $\int \kappa^n\, ds$ *for* $n \geq 3$. *In particular,* $\int \kappa^3\, ds$ *is* not *conserved in general: one computes* $\frac{d}{dt}\int \kappa^3\, ds = 3\int \kappa_s^3\, ds \neq 0$.

Proof. The conservation of $\mathcal{I}_n$ follows from the complete integrability of the mKdV Equation (2) via the Lax pair, which gives infinitely many commuting conserved quantities; see [25,26]. Conservation of $\mathcal{I}_0$ also follows from the Gauss–Bonnet theorem: for a planar curve with total turning angle $\int \kappa\, ds$ and winding number one, the total turning is 2π for a simple closed curve and is preserved by any local flow that preserves arc length and planarity. Modern accounts of mass, momentum, and energy conservation in the KdV equation are given by Ali and Kalisch [24]. Finally, to see that $\int \kappa^3\, ds$ is not conserved, differentiate under the integral using the mKdV equation $\kappa_t = \kappa_{sss} + \frac{3}{2}\kappa^2\kappa_s$:

$$\frac{d}{dt}\int_{-\infty}^{\infty} \kappa^3\, ds = 3\int_{-\infty}^{\infty} \kappa^2\kappa_t\, ds = 3\int_{-\infty}^{\infty} \kappa^2\left(\kappa_{sss} + \tfrac{3}{2}\kappa^2\kappa_s\right) ds.$$

The second integrand $\kappa^4\kappa_s = \frac{1}{5}(\kappa^5)_s$ is an exact derivative and vanishes. For the first, integrate by parts twice (boundary terms vanish by decay):

$$\int \kappa^2\kappa_{sss}\, ds = -\int 2\kappa\kappa_s\kappa_{ss}\, ds = \int \kappa_s^3\, ds.$$

Using $2\kappa_s\kappa_{ss} = (\kappa_s^2)_s$ in the second integration by parts. Hence

$$\frac{d}{dt}\int_{-\infty}^{\infty} \kappa^3\, ds = 3\int_{-\infty}^{\infty} \kappa_s^3\, ds \neq 0,$$

in general, which confirms that $\int \kappa^3\, ds$ is not conserved. □

Corollary 2 (Elastica energy of the one-soliton)**.** *For the one-soliton (7) with amplitude* $2B$,

$$\mathcal{I}_1 = \int_{-\infty}^{\infty} 4B^2 \operatorname{sech}^2(Bs)\, ds = 4B^2 \cdot \frac{2}{B} = 8B. \tag{30}$$

The elastica energy is proportional to the soliton amplitude B, *independent of the speed* B^2.

Proof. $\int_{-\infty}^{\infty} \operatorname{sech}^2(Bs)\, ds = \frac{1}{B}[\tanh(Bs)]_{-\infty}^{\infty} = \frac{2}{B}$. □

Remark 10 (Geometric significance of the conservation laws)**.** *The three conserved quantities govern distinct geometric aspects of the loop soliton surface.*

(i) Conservation of $\mathcal{I}_0 = 2\pi$ *fixes the loop topology: the self-intersection and* 2π *winding cannot be destroyed by the flow.*

(ii) Conservation of $\mathcal{I}_1 = 8B$ *freezes the amplitude* B *and with it the loop height* $y_\infty = 2/B$, *the speed* B^2, *and the mean curvature at the crossing* $H(0) = -(1 + B^4)B$.

(iii) Conservation of $\mathcal{I}_2$ *constrains perturbations to remain near the soliton in function space, providing Lyapunov-type control on the surface geometry.*

Remark 11 (Consistency with the mKdV hierarchy)**.** *The conserved density* $\kappa_s^2 - \frac{1}{4}\kappa^4$ *is consistent with the standard mKdV hierarchy. Under the substitution* $u = \sqrt{3/2}\,\kappa$ *(which maps (2) to the standard mKdV equation* $u_t = u_{sss} + u^2 u_s$*), one has*

$$\kappa_s^2 - \tfrac{1}{4}\kappa^4 = \tfrac{2}{3}u_s^2 - \tfrac{1}{4}\cdot\tfrac{4}{9}u^4 = \tfrac{2}{3}\Big(u_s^2 - \tfrac{1}{6}u^4\Big),$$

which is proportional to the standard third mKdV conserved density $u_s^2 - \frac{1}{6}u^4$ *for* $u_t = u_{sss} + u^2 u_s$*. This confirms that the coefficient* $-\frac{1}{4}$ *in* $\mathcal{I}_2$ *is correct.*

Remark 12 (Comparison of conservation laws)**.** *The KdV hierarchy conserves* $\int \kappa\, ds$*,* $\int \kappa^2\, ds$*, and higher-order combinations involving* κ_s*,* κ_{ss}*, etc. (not simply* $\int \kappa^n\, ds$ *for* $n \geq 3$*, which are* not *conserved in general—see Theorem 10). The NLS hierarchy (Hasimoto flow) conserves* $\int \kappa^2\, ds$*,* $\int \kappa^2\tau\, ds$*, etc.–different invariants involving the torsion* τ*. The linearized flow has no non-trivial conservation laws. This hierarchy of invariants distinguishes the three frameworks at the integrable-systems level.*

Three phenomena distinguish the KdV curve flow from both the linear and Hasimoto frameworks:

(1) **Loop topology.** The KdV soliton generates a curve with a genuine loop (self-intersection), a feature absent in both the linearized cylinder and the VFE elastica. The loop produces the factor $D = 1 + B^4 \sin^2\theta$, which varies along the surface and makes the geometry non-uniform in a way absent from the other two frameworks.

(2) **The $D^{3/2}$ denominator.** The mean curvature $H = -(1 + B^4)\kappa/(2D^{3/2})$ carries the factor $D^{3/2}$, which is not present for the VFE stationary soliton ($H = -\kappa/2$) or the linearized cylinder ($H = \text{const}$). This factor suppresses the mean curvature at the loop tips (where D is large) relative to the crossing point, creating a geometric ridge structure.

(3) **Non-elementary Willmore energy with sharp asymptotics.** For the *VFE* stationary soliton (Hasimoto flow), the Willmore integral reduces to an elementary combination of sech-powers, is therefore finite, and carries no position-dependent factors; its B-dependence is fixed by the sech-integral alone. For the KdV loop soliton surface, the $D^{5/2}$ denominator in the Willmore integrand involves $\operatorname{sech}^2(Bu)\sin^2\theta(u)$ and does not simplify to a standard integral. However, as established in Theorem 9, the large-B asymptotics is rigorously $\mathcal{W} \sim \frac{2}{3}B^7 T$, a genuinely new scaling determined by the boundary-layer structure at $u = 0$.

9. Examples

We construct the loop soliton surface step by step for three values of the amplitude parameter B, illustrating how the geometry changes. In each case, we follow six explicit steps: specify the curvature soliton, compute the tangent angle, derive the explicit curve, lift to the surface, compute the fundamental forms, and evaluate the curvatures.

Given $B > 0$, the loop soliton surface $\mathbf{r}(u,t) : ([-L, L]) \times [0, T] \to \mathbb{E}^3$ is built as follows.

Step 1 (KdV soliton curvature): $\kappa(u) = 2B\operatorname{sech}(Bu)$, where $u = s + B^2 t$ is the co-moving variable.

Step 2 (Tangent angle): $\theta(u) = \int_0^u \kappa\, du' = 2\arctan(\sinh(Bu))$. Setting $c = \operatorname{sech}(Bu)$ and $h = \tanh(Bu)$, we have $\cos\theta = 2c^2 - 1$, $\sin\theta = 2ch$.

Step 3 (Loop soliton curve):

$$x(u) = \frac{2\tanh(Bu)}{B} - u, \qquad y(u) = \frac{2}{B}(1 - \operatorname{sech}(Bu)). \tag{31}$$

Vertical tangents ($\cos\theta = 0$) at $u^* = \pm\ln(1 + \sqrt{2})/B \approx \pm 0.881/B$; loop height $y_\infty = 2/B$.

Step 4 (Surface): $\mathbf{r}(u,t) = (x(u) + B^2 t,\ y(u),\ t)$.
Step 5 (Fundamental forms):

$$E = 1, \quad F = B^2(2c^2 - 1), \quad G = 1 + B^4, \quad D = 1 + B^4 \sin^2\theta.$$

$$L = -\frac{2Bc}{\sqrt{D}}, \quad M = 0, \quad N_{\mathrm{II}} = 0.$$

Step 6 (Curvatures):

$$K = 0, \qquad H = -\frac{(1+B^4)\cdot 2Bc}{2D^{3/2}} = -\frac{(1+B^4)Bc}{D^{3/2}}.$$

At the crossing ($u = 0$, $\theta = 0$, $c = 1$, $D = 1$): $H_{\max} = -(1 + B^4)B$. At the tips ($u = u^*$, $\theta = \pi/2$, $D = 1 + B^4$): $H_{\mathrm{tip}} = -(1 + B^4)Bc(u^*)/[(1 + B^4)^{3/2}] = -Bc(u^*)/\sqrt{1 + B^4}$.

Example 1. *With $B = 1/2$, soliton speed $B^2 = 1/4$, amplitude $\kappa_{\max} = 1$.*

Curve (from Step 3):

$$x(u) = 4\tanh(u/2) - u, \qquad y(u) = 4(1 - \operatorname{sech}(u/2)).$$

Vertical tangents at $u^* = \dfrac{\ln(1+\sqrt{2})}{B} = \dfrac{\ln(1+\sqrt{2})}{1/2} \approx 1.763$*; loop height* $y_\infty = 4$*. The loop is broad and low-curvature.*

Surface (Step 4): $\mathbf{r}(u,t) = (x(u) + \frac{t}{4},\ y(u),\ t)$.

Fundamental forms (Step 5), using $B^4 = 1/16$*:*

$$E = 1, \quad F = \tfrac{1}{4}(2c^2 - 1), \quad G = \tfrac{17}{16}, \quad D = 1 + \tfrac{1}{16}\sin^2\theta.$$

Since $B^4 = 1/16 \ll 1$*, we have* $D \approx 1$ *everywhere.*

Curvatures (Step 6):

$$K = 0, \qquad H = -\frac{\frac{17}{16}\cdot\frac{\operatorname{sech}(u/2)}{2}}{D^{3/2}} \approx -\frac{17}{32}\operatorname{sech}(u/2).$$

Maximum $|H(0)| \approx 17/32 \approx 0.531$*. At the tips:* $c(u^*) \approx 0.707$*,* $H_{\mathrm{tip}} = -\sqrt{2/17} \approx -0.343$.

Example 2. *With $B = 1$, soliton speed $B^2 = 1$, amplitude $\kappa_{\max} = 2$.*

Curve (Step 3):

$$x(u) = 2\tanh(u) - u, \qquad y(u) = 2(1 - \operatorname{sech}(u)).$$

Vertical tangents at $u^* \approx \pm 0.881$*; loop height* $y_\infty = 2$.

Surface (Step 4): $\mathbf{r}(u,t) = (x(u) + t,\ y(u),\ t)$.

Fundamental forms (Step 5), using $B^4 = 1$*:*

$$E = 1, \quad F = 2c^2 - 1 = \cos\theta, \quad G = 2, \quad D = 1 + \sin^2\theta.$$

Curvatures (Step 6) at three key points are defined as follows.

The curvature values at the three key points are summarised in Table 1, showing the mean curvature ridge from -2 *at the crossing to* 0 *at spatial infinity.*

The exact integrand is $f(u) = (1 + B^4)^2\kappa(u)^2/(4D(u)^{5/2})$. *For* $B = 1$, *this becomes* $f(u) = 4\,\mathrm{sech}^2(u)/(1 + \sin^2\theta(u))^{5/2}$. *High-precision adaptive quadrature (error* $< 5 \times 10^{-7}$*) gives* $\mathcal{W}(\infty, T) \approx 3.532\,T$; *the convergence is documented in Table 2.*

Table 1. Curvature values at three key points of the loop soliton surface for $B = 1$, where u is the arc length parameter, θ is the tangent angle, $c = \mathrm{sech}(u)$ is the hyperbolic secant, $D = 1 + \sin^2\theta$ is the metric discriminant, and H is the mean curvature. The mean curvature forms a ridge of magnitude $|H| = 2$ at the loop crossing $u = 0$, drops to $|H| = 1/2$ at the loop tips and decays to zero in the far field.

Point	u	θ	$c = \mathrm{sech}(u)$	D	H
Crossing	0	0	1	1	-2
Tips	$\approx\pm 0.881$	$\pm\pi/2$	$1/\sqrt{2} \approx 0.707$	2	$-1/2$
Far field	$\pm\infty$	$\pm\pi$	0	1	0

Table 2. Numerical convergence of the Willmore energy half-integral $\int_0^S f(u)\,du$ for $B = 1$, computed by high-precision adaptive quadrature over increasing domains $[0, S]$. The half-integral stabilises at 1.766 for $S \geq 6$; doubling by symmetry gives $\mathcal{W}(\infty, T) \approx 3.532\,T$. The integrand at $u = 6$ is below 10^{-6}, confirming essential convergence.

Domain	Step Size	$\mathcal{W}(S,T)/T$
$[0, 4]$	$h = 0.05$	1.763
$[0, 6]$	$h = 0.05$	1.766
$[0, 8]$	$h = 0.05$	1.766

As Table 2 shows, the integral converges to $\mathcal{W}(\infty, T) \approx 3.532\,T$ *(doubling the half-integral by symmetry). The two asymptotic limits give* $2BT = 2\,T$ *(small-B formula, over-estimate at* $B = 1$*) and* $\frac{2}{3}B^7T = 0.667\,T$ *(large-B formula, under-estimate at* $B = 1$*). The value* $3.532\,T$ *lies well above both, reflecting that* $B = 1$ *sits in the crossover regime where neither asymptotic is accurate.*

9.1. Example 3: $B = 2$ *— Narrow, High-Amplitude*

Example 3. *With* $B = 2$, *soliton speed* $B^2 = 4$, *amplitude* $\kappa_{\max} = 4$.

Curve (Step 3):

$$x(u) = \tanh(2u) - u, \qquad y(u) = 1 - \mathrm{sech}(2u).$$

Vertical tangents at $u^* \approx \pm 0.440$; *loop height* $y_\infty = 1$. *The loop is tight and narrow.*

Surface (Step 4): $\mathbf{r}(u, t) = (x(u) + 4t,\, y(u),\, t)$.

Fundamental forms (Step 5), using $B^4 = 16$:

$$E = 1, \quad F = 16(2c^2 - 1), \quad G = 17, \quad D = 1 + 16\sin^2\theta.$$

At the tips ($\sin^2\theta = 1$): $D = 17$ *— large D-variation due to* $B^4 = 16$.

Curvatures (Step 6):

$$H = -\frac{17 \cdot 4\,\mathrm{sech}(2u)}{2(1 + 16\sin^2\theta)^{3/2}}.$$

Table 3 summarises the curvature values; the drop by a factor of ≈ 99 *from crossing to tips is consistent with the analytical formula:* $|H_{\max}|/|H_{\mathrm{tip}}| = D_{\mathrm{tip}}^{3/2}/c(u^*) = 17^{3/2}/(1/\sqrt{2}) = 17\sqrt{17} \cdot \sqrt{2} \approx 98.6$. *Here* $c(u^*) = \mathrm{sech}(2u^*) = 1/\sqrt{2}$ *(since* $\cosh(2u^*) = \sqrt{2}$, *which follows from* $u^* = \ln(1 + \sqrt{2})/2$

and $\cosh(\ln(1+\sqrt{2})) = \sqrt{2}$*). This is substantially larger than the factor* ≈ 10 *for* $B = 1$*, due to the large* $D_{\text{tip}} = 17$ *at* $B = 2$*.*

Table 3. Curvature values at three key points of the loop soliton surface for $B = 2$, where u is the arc length parameter, $c = \operatorname{sech}(2u)$ is the hyperbolic secant, $D = 1 + 16\sin^2\theta$ is the metric discriminant, H is the mean curvature, and the ratio $|H_{\max}|/|H|$ measures the drop in mean curvature relative to its maximum value $|H_{\max}| = 34$ at the crossing. The curvature drops by a factor of $\approx$99 from the crossing to the tips, consistent with the analytical formula $|H_{\max}|/|H_{\text{tip}}| = D_{\text{tip}}^{3/2}/c(u^*) = 17^{3/2}/(1/\sqrt{2}) = 17\sqrt{17}\cdot\sqrt{2} \approx 98.6$, and decays to zero in the far field.

Point	$\boldsymbol{u}$	$\boldsymbol{c = \operatorname{sech}(2u)}$	$\boldsymbol{D}$	$\boldsymbol{H}$	**Ratio** $\boldsymbol{|H_{\max}|/|H|}$
Crossing	0	1	1	-34	1
Tips	$\approx\pm 0.4406$	$1/\sqrt{2} \approx 0.7071$	17	≈ -0.343	$\approx$99
Far field	$\pm\infty$	0	1	0	∞

The three-dimensional surface for $B = 2$ is shown in Figure 1, which illustrates the tight loop, the rapid translation at speed $B^2 = 4$, and the sharp mean-curvature ridge at the crossing $u = 0$.

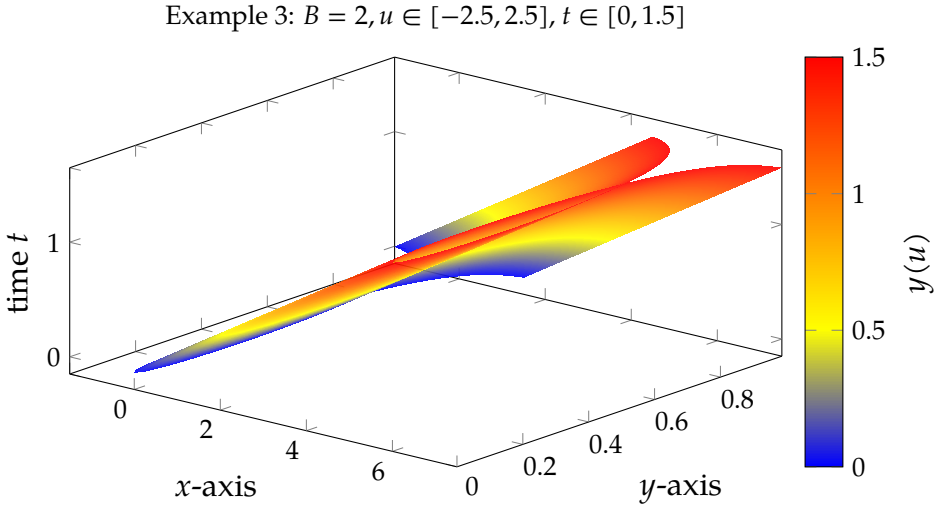


Figure 1. Example 3 ($B = 2$): narrow, high-amplitude loop soliton surface. The loop is tight (vertical tangents at $u \approx \pm 0.44$), the surface moves rapidly at speed $B^2 = 4$, and the large $D = 17$ at the tips causes a dramatic drop in mean curvature from -34 to -0.343. The colour map (`hot`, ranging from dark red at low values to bright yellow–white at high values) encodes the y-coordinate $y(u) = 1 - \operatorname{sech}(2u)$ of the surface: dark colours near $y = 0$ mark the loop crossing at $u = 0$, while lighter colours near $y = 1$ correspond to the loop tips and the asymptotic height $y_\infty = 1$.

9.2. Comparison of the Three Examples

Table 4 collects the geometric data for all three examples, confirming the trends described in Steps 1–6 above.

Remark 13. *In all three examples, the surface is a* ruled developable*: the t-parameter curves* $\mathbf{r}(u_0, t) = (x(u_0) + B^2 t,\ y(u_0),\ t)$*, for each fixed* u_0*, are straight lines (generatrices) in the constant direction* $(B^2, 0, 1)$*. These t-curves are precisely the rulings of the developable surface. This can be verified directly:* $\partial_t \mathbf{r} = (B^2, 0, 1)$ *is independent of t, so each t-curve is indeed an affine line. The ruling direction* $(B^2, 0, 1)$ *makes an angle* $\arctan(1/B^2)$ *with the time axis; as B increases, the ruling tilts further from vertical toward the x-direction. The u-parameter curves (*$t = $ const*), by contrast,*

are the loop soliton curves themselves and are not straight lines (they have non-zero curvature κ). The developable structure is thus, precisely, rulings = t-curves, base curve = u-curve.

Table 4. Geometric summary for the three examples. As B increases, the loop narrows ($u^* \propto 1/B$), the height decreases ($y_\infty = 2/B$), the crossing curvature grows as $-(1+B^4)B$, and the ratio $|H_{\max}|/|H_{\text{tip}}|$ grows rapidly due to the $D^{3/2}$ factor.

B	$\kappa_{\max}$	Speed B^2	u^*	y_∞	$H(0)$	$H(u^*)$
1/2	1	1/4	$\approx$1.763	4	$-17/32 \approx -0.531$	$-\sqrt{2/17} \approx -0.343$
1	2	1	$\approx$0.881	2	-2	$-1/2$
2	4	4	$\approx$0.440	1	-34	$-2/\sqrt{34} \approx -0.343$

10. Conclusions

We have analyzed the surface swept by the loop soliton of the KdV curve flow. The curve has closed-form parametrization $x(u) = 2\tanh(Bu)/B - u$, $y(u) = 2(1-\operatorname{sech}(Bu))/B$, and its lift to $\mathbb{E}^3$ is a flat developable ($K = 0$) whose mean curvature $H = -(1+B^4)\kappa/(2D^{3/2})$, with $D = 1 + B^4\sin^2\theta$, is concentrated on a sharp ridge along the loop crossing and decays exponentially at infinity. The principal curvatures are $-\kappa/\sqrt{D}$ and 0; all geodesics are affine lines in a flat coordinate system; and the Willmore energy on an infinite strip admits the sharp asymptotics $\mathcal{W} \sim 2BT$ as $B \to 0^+$ and $\mathcal{W} \sim \frac{2}{3}B^7T$ as $B \to +\infty$. Three geometric conservation laws inherited from the mKdV hierarchy—total turning, elastica energy $8B$, and the second mKdV invariant—are preserved by the flow. The geometric significance of the three main results is as follows. The flatness $K = 0$ combined with non-constant mean curvature is geometrically striking: flat surfaces are classically associated with developable cylinders or planes, where H is either constant or zero. Here, the loop topology forces a genuine curvature ridge of amplitude $|H(0)| = (1+B^4)B$ along the self-intersection, while the surface remains isometric to the plane. Physically, for a vortex filament confined to a plane under the localized induction approximation, this ridge represents a concentration of bending stress at the crossing point of the loop—a localised region of intense curvature embedded in an otherwise flat flow surface. The flatness $K = 0$ and the geodesic result—that the t-parameter curves are simultaneously geodesics and asymptotic lines, and that all geodesics are affine in a flat coordinate system—are consequences of the general theory of generalised cylinders (as noted in Remark 8) and are included here for completeness and explicit verification in this specific setting. The B^7 Willmore asymptotics is the most unexpected result. It arises because the loop topology introduces the factor $D^{5/2}$ in the Willmore integrand, which concentrates bending energy into a boundary layer of width $\sim B^{-2}$ near the crossing. The peak of H^2 grows as B^{10}, partially compensated by the B^{-2} width, yielding a net B^7 divergence. This places the KdV loop soliton surface in a class of its own within the theory of Willmore functionals: neither the linear cylinder (whose Willmore energy grows linearly in strip length) nor the Hasimoto soliton (whose Willmore energy is finite and elementary) exhibits this scaling.

Several questions remain open. The non-planar extension, obtained by adding a binormal component $W\,B$ to the flow, leads to a coupled KdV–mKdV system whose integrability and surface geometry are largely unexplored [8]; the two-soliton surface obtained by the Bäcklund transformation has not yet been described geometrically; the higher-order terms of the large-B Willmore asymptotics can be refined; and the question of whether non-soliton solutions of KdV produce surfaces with $K \neq 0$ remains open. Two broader programs are also suggested: the study of mean curvature flow as a companion to the KdV curve flow [28,29] and the analysis of elastica boundary value problems for loop soliton segments

following the constructive procedure of [14]. Each lies within reach of the Frenet–Serret and integrable-systems toolkit developed here.

Author Contributions: Conceptualization, A.E. and E.G.R.; methodology, A.E.; software, A.E.; validation, A.E. and E.G.R.; formal analysis, A.E.; investigation, A.E. and E.G.R.; resources, A.E.; data curation, A.E.; writing—original draft preparation, A.E.; writing—review and editing, A.E. and E.G.R.; visualization, A.E.; supervision, A.E.; project administration, A.E.; funding acquisition, E.G.R. All authors have read and agreed to the published version of the manuscript.

Funding: The authors extend their appreciation to Princess Nourah bint Abdulrahman University for funding this research under Researchers Supporting Project number (PNURSP2026R895), Princess Nourah bint Abdulrahman University, Riyadh, Saudi Arabia.

Institutional Review Board Statement: The authors hereby affirm that the contents of this manuscript are original. Furthermore, it is not published or under review for publication elsewhere in any language fully or partly.

Data Availability Statement: No new data were created or analyzed in this study. Data sharing is not applicable to this article.

Conflicts of Interest: The authors declare no conflicts of interest.

References

1. Chou, K.-S.; Qu, C. Integrable equations arising from motions of plane curves. *Phys. D Nonlinear Phenom.* **2002**, *162*, 9–33. [CrossRef]
2. Goldstein, R.E.; Petrich, D.M. The Korteweg–de Vries hierarchy as dynamics of closed curves in the plane. *Phys. Rev. Lett.* **1991**, *67*, 3203–3206. [CrossRef] [PubMed]
3. Nakayama, K.; Segur, H.; Wadati, M. Integrability and the motion of curves. *Phys. Rev. Lett.* **1992**, *69*, 2603–2606. [CrossRef] [PubMed]
4. Elsharkawy, A. Exploring Hasimoto surfaces within equiform geometry in Minkowski space. *Phys. Scr.* **2025**, *100*, 016101. [CrossRef]
5. Elsharkawy, A.; Cesarano, C.; Tawfiq, A.; Ismail, A.A. The non-linear Schrödinger equation associated with the soliton surfaces in Minkowski 3-space. *AIMS Math.* **2022**, *7*, 17879–17893. [CrossRef]
6. Hamouda, E.; Moaaz, O.; Cesarano, C.; Askar, S.; Elsharkawy, A. Geometry of solutions of the quasi-vortex filament equation in Euclidean 3-space $\mathbb{E}^3$. *Mathematics* **2022**, *10*, 891. [CrossRef]
7. Hasimoto, H. A soliton on a vortex filament. *J. Fluid Mech.* **1972**, *51*, 477–485. [CrossRef]
8. Adans, Y.F.; França, G.; Gomes, J.F.; Lobo, G.V.; Zimerman, A.H. Negative flows of generalized KdV and mKdV hierarchies and their gauge–Miura transformations. *J. High Energy Phys.* **2023**, *2023*, 160. [CrossRef]
9. Wang, X.; Kang, J.; Zhang, J.; Zhao, T.; Jin, W. Darboux transformation and loop soliton solutions for the complex space–time-shifted nonlocal short pulse equation. *Nonlinear Dyn.* **2023**, *111*, 13375–13390. [CrossRef]
10. Song, J.; Qu, C.; Yao, R. Integrable systems and invariant curve flows in symplectic Grassmannian space. *Phys. D Nonlinear Phenom.* **2017**, *349*, 1–11. [CrossRef]
11. Benson, J.; Valiquette, F. Geometric curve flows in low dimensional Cayley–Klein geometries. *J. Integr. Syst.* **2020**, *5*, xyaa003. [CrossRef]
12. Park, H.; Kajiwara, K.; Kurose, T.; Matsuura, N. Defocusing mKdV flow on centroaffine plane curves. *JSIAM Lett.* **2018**, *10*, 25–28. [CrossRef]
13. Calini, A.; Ivey, T. Integrable geometric flows for curves in pseudoconformal S^3. *J. Geom. Phys.* **2021**, *166*, 104249. [CrossRef]
14. Arroyo, J.J.; Garay, Ó.J.; Pámpano, Á. Boundary value problems for Euler–Bernoulli planar elastica. A solution construction procedure. *J. Elast.* **2020**, *139*, 359–388. [CrossRef]
15. Calini, A.; Ivey, T.; Marí-Beffa, G. Remarks on KdV-type flows on star-shaped curves. *Phys. D* **2009**, *238*, 788–797. [CrossRef]
16. Calini, A.; Ivey, T. Bäcklund transformations and knots of constant torsion. *J. Knot Theory Its Ramif.* **1998**, *7*, 719–746. [CrossRef]
17. Doliwa, A.; Santini, P.M. An elementary geometric characterization of the integrable motions of a curve. *Phys. Lett. A* **1994**, *185*, 373–384. [CrossRef]
18. Singh, H.; Hanna, J.A. On the planar elastica, stress, and material stress. *J. Elast.* **2019**, *136*, 87–101. [CrossRef]
19. Langer, J.; Singer, R. Curves in the hyperbolic plane and mean curvature of tori in 3-space. *Bull. Lond. Math. Soc.* **1984**, *16*, 531–534. [CrossRef]

20. Euler, L. *Methodus Inveniendi Lineas Curvas Maximi Minimive Proprietate Gaudentes*; Marc-Michel Bousquet & Socios: Lausanne, Switzerland, 1744.
21. Langer, J.; Singer, D.A. The total squared curvature of closed curves. *J. Differ. Geom.* **1984**, *20*, 1–22. [CrossRef]
22. Korteweg, D.J.; de Vries, G. On the change of form of long waves advancing in a rectangular canal, and on a new type of long stationary waves. *Philos. Mag.* **1895**, *39*, 422–443. [CrossRef]
23. Washimi, H.; Taniuti, T. Propagation of ion-acoustic solitary waves of small amplitude. *Phys. Rev. Lett.* **1966**, *17*, 996–998. [CrossRef]
24. Ali, A.; Kalisch, H. On the formulation of mass, momentum and energy conservation in the KdV equation. *Acta Appl. Math.* **2014**, *133*, 113–131. [CrossRef]
25. Miura, R.M.; Gardner, C.S.; Kruskal, M.D. Korteweg–de Vries equation and generalizations. II. Existence of conservation laws and constants of motion. *J. Math. Phys.* **1968**, *9*, 1204–1209. [CrossRef]
26. Ablowitz, M.J.; Segur, H. *Solitons, Nonlinear Evolution Equations and Inverse Scattering*; Cambridge University Press: Cambridge, UK, 1991.
27. Toda, M.D. (Ed.) *Willmore Energy and Willmore Conjecture*; CRC Press: Boca Raton, FL, USA, 2017.
28. Chen, B.-Y. *Total Mean Curvature and Submanifolds of Finite Type*; World Scientific Publishing Company: Singapore, 2014; Volume 27.
29. Colding, T.; Minicozzi, W.; Pedersen, E. Mean curvature flow. *Bull. Am. Math. Soc.* **2015**, *52*, 297–333. [CrossRef]
30. Haiden, F.; Katzarkov, L.; Kontsevich, M. Flat surfaces and stability structures. *Publ. Mathématiques De L'IHÉS* **2017**, *126*, 247–318. [CrossRef]
31. do Carmo, M.P. *Differential Geometry of Curves and Surfaces*; Prentice-Hall: Englewood Cliffs, NJ, USA, 1976.
32. Banchoff, T.F.; Lovett, S. *Differential Geometry of Curves and Surfaces*; A K Peters/CRC Press: Boca Raton, FL, USA, 2022.

Disclaimer/Publisher's Note: The statements, opinions and data contained in all publications are solely those of the individual author(s) and contributor(s) and not of MDPI and/or the editor(s). MDPI and/or the editor(s) disclaim responsibility for any injury to people or property resulting from any ideas, methods, instructions or products referred to in the content.